Studies on Adsorptive Behavior of Cd^{2+} on Graphene Oxide: Alternative Novel Approach

A. U. Nkwoada[1*], C. O. Alisa[1], C. K. Enenebeaku[1] and E. E. Oguzie[1]

[1]*Department of Chemistry, School of Physical Sciences, Federal University of Technology Owerri, Imo state, Nigeria.*

Authors' contributions

This work was carried out in collaboration between all authors. Authors AUN and EEO designed the study, wrote the protocol and managed the literature searches. Authors COA and CKE anchored the field study, gathered the initial data and performed preliminary data analysis. Authors NAU, COA and CKE interpreted the results and produced the initial draft. All authors read and approved the final manuscript.

Original Research Article

ABSTRACT

Certain adsorptive mechanisms and interactions often exist within linearized kinetic functions which are largely unreported. A novel inverse saturation modeling was applied to evaluate the adsorptive behavior of super-saturation, saturation, and desorptive processes on linear kinetic function plots using pseudo 1st order, pseudo 2nd order, Elovich and Intra-particle diffusion. Graphene oxide was prepared by room temperature synthesis and used as adsorbent over Cd^{2+} adsorbate. Batch adsorption process was conducted and four error functions were utilized. The sum of squares of the errors and Sum of absolute errors identified pseudo 2nd order as having the least deviation at 0.113 and 0.337 respectively. The modelled pseudo 1st order reaction had $R^2 = 0.985$ while the inverse saturation model had R^2 value of 0.998, both been a better data fit than non-modelled pseudo 1st order R^2 at 0.917. The slower reaction kinetics in pseudo 1st order was due to super-saturation during adsorption as shown by inverse saturation point. The correlation coefficient of modeled kinetic plot of pseudo 2nd order, Intra particle diffusion and Elovich had $R^2 = 1$. The

---

*Corresponding author: Email: chemistryfrontiers@gmail.com;

Elovich inverse saturation plot showed that the graph was an L-isotherm type indicating progressive saturation. The rate determining step experienced by Intra-particle diffusion was accommodated by wide range of inverse saturation plots showing adsorption, supersaturation and desorption as points of greatest influence. The inverse saturation plot of pseudo 2nd order plot had absolute slope of 2.656 and large intercept of 24.815 driving it's faster reaction kinetics. Hence, the inverse saturation point modelling provided a much better interpretation of adsorptive behavior of graphene oxide adsorbent over Cd^{2+} adsorbate.

1. INTRODUCTION

Understanding the adsorptivity of graphene oxide (GO) has provided practical applications to adsorptive phenomena. In GO, for Instance, the precursor size affects energy performance ability, while synthesis affects structures and sorption surface area [1,2]. As a substrate for array of chemical transformations; GO can be synthesized into graphene sheets, layered graphene oxide and sponge-like graphene oxide. In addition, several other synthetic routes are on the increase [3,4]. Brodie and Hummers have been reported severally as the common methods of GO preparation [5]. Researchers, however, has continued to explore improved and modified Hummers method for GO synthesis alongside microwave assisted approach [6,7,8]. Remarkably, scaling up of GO and production of high purity GO was achieved by cell dialysis and dead-end filtration. Additionally, efficacy of the oxidation process was obtained by removing $NaNO_3$ from Hummers approach, while increasing the amount of $KMnO_4$ to yield hydrophilic oxidized graphene oxide [9, 10]. Recent advances in GO studies, have shown that graphene oxide can remove organic and inorganic toxic pollutants from wastewater by means of adsorption [11,12]. Interestingly, the application of GO for removal of heavy metals (Cu^{2+}, Co^{2+}, Cd^{2+}, Zn^{2+}, Ni^{2+} Pb^{2+}) has been extensively studied and are well reported [13, 14]. Similarly, ultrasonic assisted adsorption of Cd, Pb, Cu and Ni by 2, 2-dipyridylamine modified GO with silica composites has been studied. The result showed GO effective performance as adsorbent for Cd, Cr, Pb, Zn and Ni removal from aqueous solutions [14,15]. Furthermore, metal adsorption by GO can be improved because they basal planes and edges of GO encloses modifiable functional groups (epoxide, hydroxyl, carbonyl ad carboxyl). These functional groups can then be adapted for specific metal adsorbate (Cd, Pb and Cu) and the GO absorbent [16]. As a consequence, certain mechanism and interactions could also be driving kinetic steps towards other hidden non-linearized adsorptive behavior.

Cadmium (Cd^{2+}) is a heavy metal, which when accumulated in the human body has a high toxicity potential and longer exposure duration [17]. On the other hand, GO adsorbents in the form of modified carbon and other carbonized materials have effectively adsorbed Cd^{2+} metal [18,19,20,21]. Hence, graphene oxide sorption studies are significant in determining adsorption behavior of the improved adsorbent and target metal adsorbate [21,22,23,24].

However, these studies were often evaluated using pH, ionic strength and dosage amount plotted on a linearized kinetic function. These linearized kinetic functions are limited by inability to predict non-compliant data and graphs as adsorptive behavior. Thus certain other mechanism and interactions could also be driving kinetic steps and may have been unreported. Moreover, the understanding of such unique behavior would be advantageous towards the sorptive behavior of materials in industrial applications. Hence a study was designed to predict these unreported adsorptive behaviors such as super-saturation point, saturation point, adsorptive and desorptive ranges during sorption process using inverse saturation point modeling. The model was compared to linear kinetic isotherms in order to identify the best adsorbate absorptive behavior of Cd^{2+}. The scope of the work was limited to physical characterization using atomic absorption spectroscopy.

2. MATERIALS AND METHODS

Analytical grade reagents of H_2SO_4, $NaNO_3$, H_2O_2 of 99% purity and graphite flake were obtained from a standard laboratory. Double distilled water was prepared and utilized in all aqueous solution preparations. All experiments were carried out using 250, 500 and 1000 mL airtight Erlenmeyer flask. The Concentrations

were diluted with 0.1 M HCl and 0.1 M NaOH. All experiments were run in triplicates and average values were reported as batch readings.

2.1. Preparation of Graphene Oxide

Using previously reported preparation, graphite flake of about 1.5 g was slowly introduced into a 250 ml Erlenmeyer flask having 69 mL of H_2SO_4 that was charged with a magnetic stirring bar. The reaction (solution) was maintained at 0 - 5 °C using ice bath immersion until a black slurry (viscous) of graphite powder was formed. The slurry mixture was kept below 3°C and 1.5 g of $NaNO_3$ was slowly added over a period of 20 minutes. The mixture was then allowed to equilibrate at room temperature and continuously stirred further for 1 hr. About 120 mL of the double distilled water was added during which 30 minutes stirring was performed until the temperature reached 90°C. Then the reaction mixture was poured into a 1000 mL flask containing 300 mL of double-distilled water. Then 10 mL of H_2O_2 was slowly added and immediate colour change of the solution from dark-brown to yellow was observed. Using a 0.22 μm filter membrane, the solution was filtered and re-washed severally in water until a neutral pH of 7.0 was obtained. The soluble GO obtained was dried and placed in a desiccator for 24 hours at room temperature and kept stored in ambient environment [21,22,23,24].

2.2 Batch Adsorption Studies of Cd^{2+}

Batch adsorption of Cd^{2+} onto the GO was carried out in a 250 mL airtight Erlenmeyer flask containing 20 mL of known concentration (15 ppm) of the solution and an accurately weighed amount of the adsorbent. The reaction mixture in the flask was agitated by magnetic shaker at a constant speed of 150 rpm for 10 mins. The mixture was centrifuged at 10,000 rpm at room temperature (298K) and pH (6.5). The effect of contact time (10, 20, 40, 60, 80,120, 150, 180 min) and adsorbent dosages (10, 20, 30, 40, 50, 60, 80 100 mg) were evaluated. The flask containing the samples were retrieved from the shaker at the predetermined time intervals, filtered and the final concentrations of Cd^{2+} in the clear solutions determined using Atomic Adsorption Spectrometer [14,18].

The Cd (II) ion adsorption capacity at time t (qt), in mg/g, was calculated using equation 1 below

$$qt = [(Co - Ct)] \times \frac{v}{w} \qquad (1)$$

Where *Co* (mg/L) is the initial Cd (II) ion concentration, *Ct* (mg/L) the Cd (II) ion concentration at time t, *W* (g) the adsorbent mass and *V*(L) the volume of Cd (II) ion solution.

2.3 Kinetic Isotherm Modeling

The design of efficient adsorption processes requires equilibrium adsorption data for kinetic isotherm modeling. The adsorptive behavior of Cd^{2+} over GO was modeled using Pseudo 1st order, Pseudo 2nd order, and Elovich and intra-particle diffusion as shown in Table 1.

The obtained data were fitted into their linear functions. The equation generated from the modeled data was further used to determine their kinetic parameters and inverse saturation points respectively.

2.4 Inverse Saturation Point Modeling (P)

For the first time, inverse saturation point on adsorptive experiment was utilized. The obtained linear kinetic isotherm equations were used to determine the predicted values at selected extended time for pseudo 1st order, pseudo 2nd order, Intra-particle diffusion and Elovich function. Then the values obtained were used to calculate the inverse saturation point of each of the kinetic isotherm function respectively. To obtain the inverse saturation point, arbitrary extension of experimental time (x) was chosen to be 200, 250, 300, 350 and 400 minutes for each kinetic function respectively. So that x = 200, 250, 300, 350 and 400 minutes. The values of x were now substituted into the linear model equation to obtain y values respectively. The calculated % fraction of a preceding and succeeding y value gives the inverse saturation percentage.

2.5 Error Analyses

Four error functions (SSE, SAE, MPSED, HYBRID) were utilized to evaluate the suitability of each kinetic isotherm equation to the experimental data sets and modeled data sets [25,26,27,28] as described in Table 2.

3. RESULTS AND DISCUSSIONS

3.1 Kinetic Isotherm

The linearized kinetic graphs were plotted as seen in Fig. 1. The visual inspection of their residual plots using Origin software showed no

Table 1. linear forms of pseudo 1st order, pseudo 2nd order, Elovich and Intra-particle diffusion

Kinetic model	Linearized form	Plots	Slopes	Intercept
Pseudo-1st order	$\log(qe - qt) = \log(qe) - \dfrac{k1t}{2.303}$	Log (qe-qt) vs t	$-\dfrac{K1}{2.303}$	$\log(qe)$
Pseudo-2nd order	$\dfrac{t}{qt} = \dfrac{1}{kqe2} + \dfrac{1t}{qe}$	$\dfrac{t}{qt}$ vs t	$\dfrac{1}{qe}$	$\dfrac{1}{qe}$
Intra-Particle diffusion	$qt = Kdt^{1/2} + C$	qt vs $t^{1/2}$	K_d	C
Elovich	$qt = \dfrac{1}{\beta}\ln(\alpha\beta) + \dfrac{1}{\beta}\ln(t)$	qt vs $\ln(t)$	$\dfrac{1}{\beta}$	$\dfrac{1}{\beta}\ln(\alpha\beta)$

Table 2. Error functions with definition and formula

Error function	Definition	Formula
Sum of the squares of the errors (SSE)	SSE is the error function that increases as the concentration increases	$SSE = \sum(qc - qe)2$
Sum of Absolute errors (SAE)	SAE is the error function that identifies the difference between predicted and observed value for regression.	$\displaystyle\sum_{i=1}^{p}[qe - qc]\,i$
Marquardt's Percent standard deviation (MPSED)	MPSED is the error function that allows for the number of degrees of freedom of the system.	$MPSD = \sqrt{\dfrac{\Sigma\left[\frac{qe-qc}{qe}\right]2}{N-P}}$
The Hybrid fractional error function (HYBRID)	HYBRID error functions is an improved SSE that considers lower concentration with included divisor	$HYBRID = \dfrac{1}{N-P}\Sigma\left[\dfrac{qe-qc}{qe}\right]100$

definite pattern or trend; an indication of a good kinetic fitting. The figure depicted that only the dependent variable (y value) of pseudo 2nd order was increasing as time increased. This indicated a positive Cd^{2+} absorption interaction. While the Pseudo 2nd order, Elovich function and intra-particle diffusion rates were decreasing as time increased. Moreover, the applicability of pseudo 2nd order reaction provided a better experimental and calculated fit for the data when compared with pseudo 1st order as indicated by R^2 (0.995). On the other hand, the concentration of Cd^{2+} adsorbed, shown by qe calculated in pseudo 1st order (see Table 3) was significantly larger than pseudo 2nd order (281.19 > 0.388 mg/g), likewise their initial adsorption rates (0.388 > 0.040 mg/g). However, the pseudo 1st order absorption constant (K_1) was considerably low at 0.012 $g.mg^{-1}$. Additionally, the adsorption rate constant of pseudo 2nd order at 0.283 $g.mg^{-1}min^{-1}$ showed a faster reaction kinetics.

The Intra-particle diffusion and Elovich appear saturated when $t^{1/2}$ was 9 and dt were 4.4 (equivalent of 80 mins) respectively and with similar R^2 values. Again, the correlation coefficient of Elovich and Intra-particle diffusion was lower than pseudo 1st and 2nd order R^2 functions although their plots did not pass through the origin

Moreover, Intra-particle diffusion intercept C (0.800 mg/g) was at low value (< 1), which showed that different rate determining steps were involved in the adsorption process. Similarly, the small α value of Elovich (0.184) confirmed a slow initial adsorption process, while the β value showed that 0.13g (i.e. 7.874g/60 min) would desorb in a second indicating a faster desorption process. These unseen "hidden" different rate-determining step in Intra-particle diffusion, faster desorption kinetics in Elovich and faster reaction kinetics in pseudo 2nd order, and slower kinetics in pseudo 1st order are never visualized in linearized models but interestingly was detected by our model as seen in Fig. 2 and section 3.2.

The statistical error functions can be indicative of good isotherm models when applied to kinetic studies. In the experiment, the pseudo 2nd order gave the least deviation in SSE and SAE error functions; a good agreement with its correlation coefficient. The error functions of pseudo 1st

order were generally high. This indicated high variations of data obtained. It confirmed the disparity between q_e calculated and q_e experimental in pseudo 1st order and its unfitness to describe the process as compared to pseudo 2nd order kinetics. Generally, the Elovich and Intra-particle diffusion had low values for all their studied kinetic error functions. However, MPSED showed only Elovich provided a better fit for data while HYBRID, SSE and SAE suggested Intra-particle diffusion provided acceptable deviations. Hence, the result proposes the suitability of data in the following order: pseudo 2nd order > intra-particle diffusion > Elovich > pseudo 1st order.
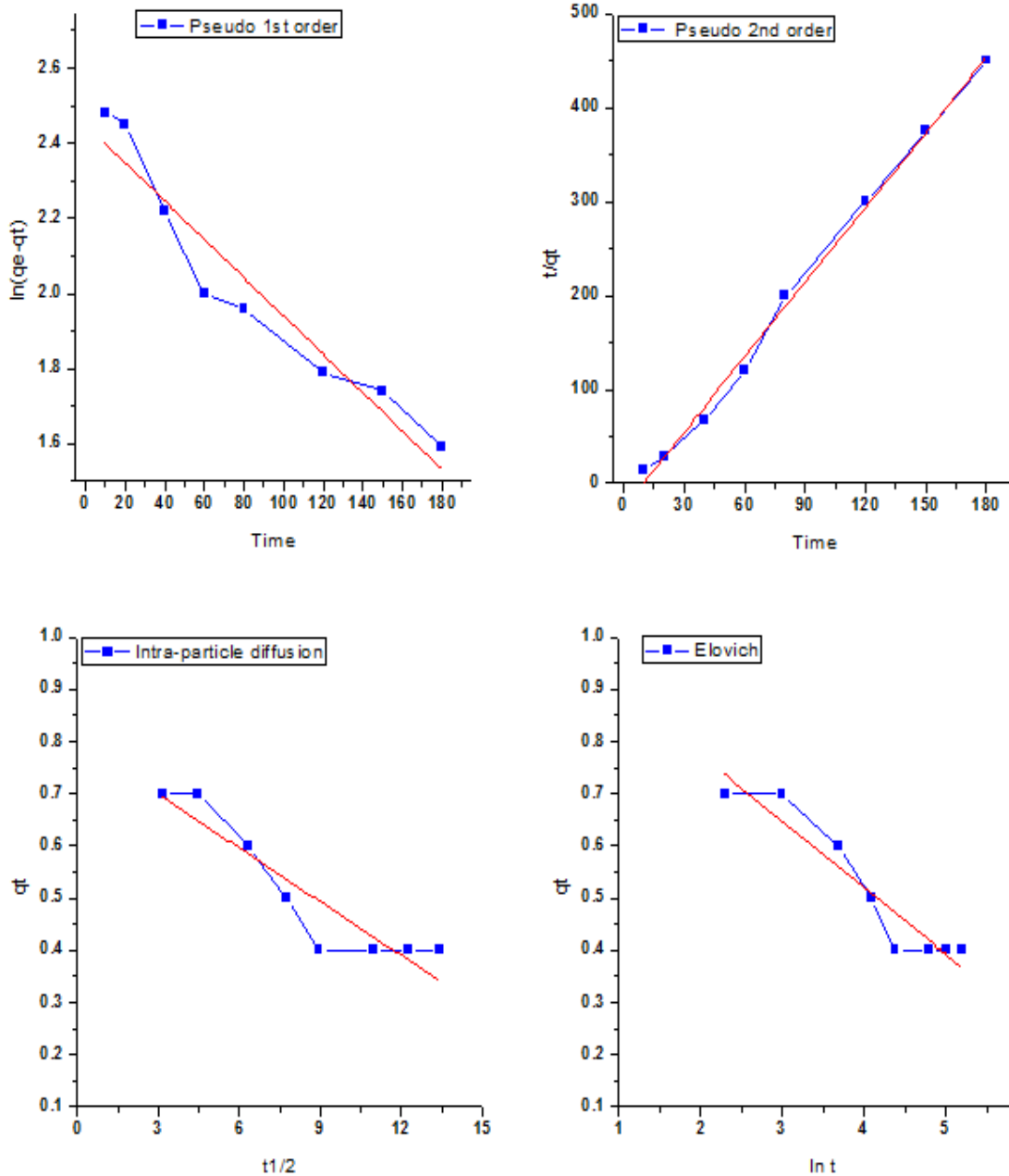

Fig. 1. linearized graphs of kinetic isotherms

Table 3. The kinetic isotherm constants for adsorption of Cd^{2+} on GO with error deviations.

	Pseudo 1st order		Pseudo 2nd order		Intra-particle diffusion		Elovich	
	qe (exp) (mg/g)	0.388	H ($mg.g^{-1}min^{-1}$)	0.040	-		-	
	K_1 ($g.mg^{-1}$)	0.012	K_2 ($g.mg^{-1}min^{-1}$)	0.283	K_{id} (mg/g/min)	-0.034	α ($mg.g.mg^{-1}$)	0.184
	qe (cal) (mg/g)	281.19	qe (cal) (mg/g)	0.377	C (mg/g)	0.800	β ($g.min^{-1}$)	7.874
	R^2	0.917	R^2	0.995	R^2	0.839	R^2	0.886
SSE	7.8 X 10^4		0.113		0.695		59.136	
SAE	280.80		0.337		0.766		7.69	
MPSED	361.85		4.213		10.075		0.436	
HYBRID	1.8 X 10^4		168.5		16.68		19.532	

Table 4. Inverse saturation point evaluation of pseudo 1st and 2nd order function

Pseudo 1st order: y = -0.0051x + 2.4499 (linear model)			Pseudo 2nd Order: y = 2.6561x -24.8153 (linear model)		
Time (mins)(x)	y value	P (%)	Time (mins)(x)	y value	P (%)
200	1.429	121.6	200	506.4047	79.2
250	1.175	127.8	250	639.2097	82.8
300	0.919	138.2	300	772.0147	85.3
350	0.665	144.8	350	904.8197	87.2
400	0.459		400	1037.6247	

Table 5. Inverse saturation point evaluation of intra-particle diffusion and Elovich

Intra-particle diffusion: y = -0.0341x + 0.8009 (linear model)			Elovich: y = -0.12736x + 1.0292		
Time (qt)(x)	y value	P (%)	Time (qt)(x)	y value	P (%)
15	0.2894	243.4	15	-0.8803	58.1
20	0.1189	-230.4	20	-1.5168	70.4
25	-0.0516	23.2	25	-2.1533	77.2
30	-0.2221	56.57	30	-2.7898	81.4
35	-0.3926		35	-3.4263	

3.2 Kinetic Inverse Saturation Point Modeling

The results of inverse saturation point determination for pseudo 1st order and pseudo 2nd order experimental data are shown in Table 4 while Elovich and Intra-particle diffusion is depicted in Table 5. Observation of the two tables showed that only pseudo 2nd order reaction had a positive slope of 2.656 while the other three functions had a negative slope.

3.2.1 X value

The extended time values which are the independent variable ranged from 200 to 400 for pseudo 1st order and pseudo 2nd order reaction. While the same values were converted to ($t^{1/2}$) in intra-particle diffusion and (ln t) in Elovich function equivalently. The range was selected to cover longer duration of experimental runs. Which can be seen in section 2.2 as effective contact time.

3.2.2 Y value

The y value represents the dependent variable which is the amount adsorbed per unit time. The values of pseudo 1st order adsorbed ranged from 0.459 to 1.429 compared to pseudo 2nd order ranging from 506 to 1037. However, the amount adsorbed decreases in pseudo 1st order but increased in pseudo 2nd order correlating their previous behavior in section 3.1 as having negative and positive energetic interaction respectively.

The amount adsorbed as shown in Elovich function and intra-particle diffusion decreased as their time increases. However, the values had negative results which showed that some kind of interaction may be competing with their kinetics. This interference was clearly seen when the graph was plotted in Fig. 2.

3.2.3 P value

The P value represents the inverse saturation points for each function and the graph was plotted in Fig. 2. The modelled pseudo 1st order reaction showed that the kinetic plot was linear with R^2 value of 0.985 while the inverse saturation model had R^2 value of 0.998. This depicted that our modeled pseudo 1st order produced a better experimental fit for data (compared to non-modeled at 0.917). This can

be seen in Fig. 1. above. while the inverse saturation point model produced a much better R^2 at 0.998 than both modeled and non-modeled data [26].

Additionally, the slower reaction kinetics of pseudo 1st order can be seen from the slope with absolute value of 0.0049. however, pseudo 1st order experienced super saturation since y value was greater than 100% and increased geometrically. Hence it would be suggested that this super saturation slowed down the adsorption kinetic process, hence a small absolute slope of 0.0049 and small intercept of 2.399. Therefore, our inverse saturation model produced a better result interpretation than normal kinetic function plots and allows researchers to make a well informed decision [26]. Similarly, analogous improvement in determining cadmium ions at low concentrations was observed using magnetic graphene nano-particles to adsorb cadmium ions. The method gave good precision and accuracy, rapid adsorption rates for the target analytes and high pre-concentration factor [28].

The pseudo 2nd order reaction kinetic data as obtained was modelled as also seen in Fig. 2. The R^2 of modelled kinetic plot was 1, depicting a perfect fit while the inverse saturation plot was at 0.969. Thus, the modelled kinetic plot ($R^2 = 1$) provided a perfect fit for acquired data points than normal kinetic plots (0.995) but showed no significant difference between the R^2 of inverse saturation point at 0.969. Moreover, its faster reaction kinetics when compared to pseudo 1st order reaction was shown by absolute slope of 2.656 and intercept of 24.815. Similarly, previous researchers have also shown that using graphene oxide as adsorbent for Cd^{2+} ions indicated pseudo-2nd order as the better fitting model for cadmium adsorption over graphene oxide derivate(s); a correlation with our study results [29,30].

On the order hand, pseudo 2nd order did not experience any super-saturation, since y values were below 100%. However, it increased geometrically from 79.2 to 87.2 and the curvature of the graph also indicated that it may eventually reach saturation at 100% and curve downwards. A concave shape of L-isotherm type showing a progressive saturation of the solid [1, 26]. Hence it would be concluded that inverse model gave a better data fit and interpretation than normal kinetic plots.
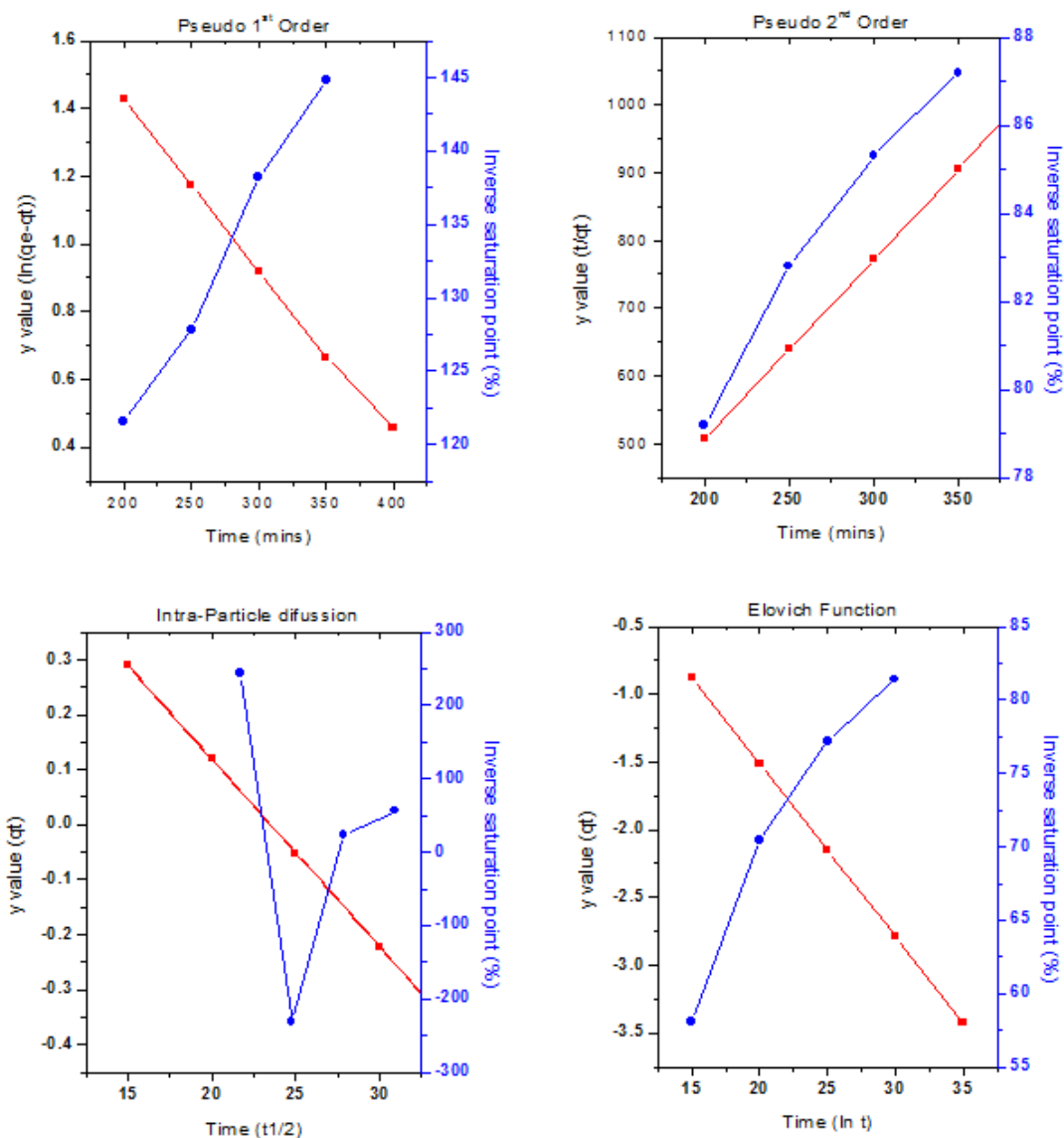
Fig. 2. modeled kinetic plot and inverse saturation model

Interestingly in section 3.1, it was identified from the intercept value of Intra-particle diffusion (0.800 mg/g < 1) that a rate-determining step was involved. Observation in Fig. 2 revealed an obstructed adsorption kinetic process when t = 25 and 27.5 respectively. The result indicated that these two points had the greatest influence on the reaction, hence the correlation between the rate determining step and earlier prediction of normal kinetic plots. on the contrary, the modelled kinetic plot had an R^2 perfect at 1 while the R^2 of modelled inverse saturation plot was negative at -0.438. This confirmed that our modelled kinetic plot provided a better experimental data fit than normal kinetic plot of $R^2 = 0.839$ in Table 3. while the negative R^2 of modelled inverse saturation showed the sensitivity of inverse saturation plot to absorptive behavior such as were several rate determining steps are involved. This is known as S isotherm; a sigmoidal behavior involving two opposing mechanisms [1, 31]. Then again, the y values of intra-particle diffusion showed a wide range of absorptive behaviors exhibited. When y = 243.4 there was super saturation, when y was - 230.4 the process had desorption while adsorption

occurred at 23.2 and 56.57. This behavior was confirmed by a negative slope of -6.1378 and large intercept at 161.293. Therefore, it was predicted that both adsorption, desorption and super saturation occurred in inter-particle diffusion, and seen in normal kinetics as rate determining step. This behavior is analogous to fluorescence quenching in some materials [1, 32]. Thus our model gave a better adsorptive behavior and perfect experimental fit for data plots.

The Elovich function also experienced faster desorption kinetics as explained in section 3.1. This can be seen in the decrease of its y value from -0.8803 to -3.4263. The graph would be seen been linear in Fig. 2. The graph had a negative slope of -0.1273 and small intercept of 1.029 depicting negative relationship (desorption) and small differences in desorbed amount. The plotted y value against x in Fig. 2 showed that a perfect correlation coefficient ($R^2 = 1$) was obtained while the modeled inverse saturation point with R^2 of 0.919. Thus both our modeled kinetic graph and modelled inverse saturation graph provided a better correlation coefficient than normal kinetic plot ($R^2 = 0.886$). On the contrary, the P value showed that only adsorption occurred and did not experience any super-saturation nor desorption. however, since y values were increasing geometrically towards 100%, the curvature of the graph suggests that it may eventually reach saturation and curve downwards as seen in pseudo 2nd order reaction. This idea was supported by its slope of 1.532 and large intercept of 37.26, suggesting faster reaction kinetics. It takes a concave shape of L-isotherm type showing a progressive saturation of the solid. [1,32] Thus it was identified that our modeled kinetic graph gave a better data fit and interpreted the desorptive behavior. Albeit, the inverse saturation point may experience desorption at some point.

4. CONCLUSION

There is the ever increasing need to remove toxic levels of Cd^{2+} from the environment using adsorbent materials such as graphene oxide [33,34,35]. The application of Graphene oxide as adsorbent in this study for removal of Cd^{2+} was successful using batch adsorption process. The Correlation coefficient R^2 of pseudo 2nd order demonstrated the best fit among the other kinetic functions. The modelled kinetic function gave a near perfect fit for all kinetic functions. The inverse saturation modelling

identified the adsorptive behavior of graphene oxide over Cd^{2+}. Hence, it demonstrated that adsorption process could quickly experience super-saturation, desorption and adsorption; analogous to fluorescence quenching at different times in same experiment. This may occur due to some order adsorptive mechanism, interactions or factors which linearized functions are unable to detect and researchers do not report. Hence, it is recommended that the application of inverse saturation point evaluation for the determination of adsorbate behavior over the adsorbent in aqueous solutions be determined and reported alongside kinetic models.

COMPETING INTERESTS

Authors have declared that no competing interests exist.

REFERENCES

1. Limousin G, Gaudet J, Szenknect S, Charlet L, Barthe V, Krismissa M. Sorption isotherms: A review on physical bases, modeling and measurement. Applied geochemistry. 2007;22:249-275. DOI:10.1016/j.apgeochem.2006.09.010
2. Botas C, Ivarez P, Granda M, Blanco C, Santaman R, Romasanta L, Menedez R. Graphene materials with different structures prepared from the same graphite by the hummers and brodie methods. Carbon. 2013;65:156-164. DOI:10.1016/j.carbon.2013.08.009
3. Minh-Hai T, Cheol-Soo Y, Sunhye Y, Ick-Jun K, Hae K. Influence of graphite size on the synthesis and reduction of graphite oxides. Current applied physics. 2014;14: S74-S79. DOI:10.1016/j.cap.2013.11.038
4. Sajjad S, Ahmed K, Anum I. Modifications in development of graphene oxide synthetic routes. Chemical Engineering Journal. 2016;294:458-477. DOI:10.1016/j.cej.2016.02.109
5. Chowdhury S, Balasubramanian R. Recent advances in the use of graphene family nano adsorbents for removal of toxic pollutants from wastewater. Advances in Colloid and Interface Science. 2014;204:35-56. DOI:10.1016/j.cis.2013.12.005
6. Chen J, Yao B, Li C, Shi G. An improved hummers method for eco-friendly

synthesis of graphene oxide. Carbon. 2013;64:225-229.
DOI:10.1016/j.carbon.2013.07.055

7. Song J, Xinzhi X, Chang C. Preparation and characterization of graphene oxide. Journal of Nano Materials. Article ID: 276143. 2014;14.
DOI:10.1155/2014/276143

8. Shahriaey L, Athawale A. Grapehene oxide synthesized by using modified hummers approach. International Journal of Renewable Energy and Environmental Engineering. 2014;2(1):58-63.

9. Yuta N. Improved synthesis of graphene oxide and its application to nano composites. Okayama University e-bulletin. 2013;3:1-2.
DOI: Japanese Patent No: 2012-201088

10. Marcano D, Kosynkin D, Berlin J, Sinitskii A, Sun Z, Slesarev A, Tour J. Improved synthesis of graphene oxide. ACSNANO. 2010;4(8):4806-4814.
DOI:10.1021/nn1006368

11. Tolle F, Gamp K, Mulhaupt R. Scale-up and purification of graphite oxide as intermediate for functionalized graphene. Carbon. 2014;75:432-442.
DOI:10.1016/j.carbon.2014.04.022

12. Kyzas Z, Deliyanni E, Matis K. Graphene oxide and its application as an adsorbent for wastewater treatment. Journal of Chemical Technology and Biotechnology. 2014;89:196-205.
DOI:10.1002/jctb.4220

13. Upadhyay RS, Bhattacharya G, Saha S, Barman A, Roy S. Grape extract assisted green synthesis of reduced graphene oxide for water treatment application. Materials Letters. 2015;160:355-358.
DOI:10.1016/j.matlet.2015.07.144

14. Zare-Dorabei R, Ferdowsi M, Barzin A, Tadjarodi A. Highly efficient simultaneous ultrasonic-assisted adsorption of Pb(II), Cd(II) and Cu(II) ions from aqeous solutions by graphene oxide modified with 2-2 dipyridylamine: Central coposite design optimization. Ultrasonics Sonochemistry. 2016;32:265-276.
DOI:10.1016/j.ultsonch.2016.03.020

15. Wang X, Guo Y, Yang L, Han M, Zhao J, Cheng X. Nanomaterials as sorbents to remove heavy metals in ions in wastewater treatment. Journal of Environmental Analytical Toxicology. 2012;7(3):1-5.
DOI:10.4172/2161-0525.1000154

16. Sheet I, Kabbani A, Holail H. Removal of heavy metals using nanostructured graphite oxide, silica nanoparticles and silica/graphite oxide composite. Energy Procedia. 2014;50:130-138.
DOI:10.1016/j.egypro.2014.06.016

17. Dreyer D, Park S, Bielawski W, Ruoff R. The chemistry of graphene oxide. Chemical Society Review. 2010;39:228-240. DOI:10.1039/B917103G

18. Ivana C, Eder C, Christopher B. Simultaneous Determination of Cadmium, Lead, Copper and Mercury Ions Using Organo-functionalized SBA-15 Nano-structured Silica Modified Graphite-Polyurethane Composite Electrode. Electroanalysis. 2010;22:61-68.
DOI:10.1002/elan.200900167

19. Mubarak N, Sahu J, Abdullah E, Javakumar N, Ganesan P. Microwave assisted multiwall carbon nanotubes enhancing Cd(II) adsorption capacity in aqeous media. Journal of Industrial and Engineering Chemistry. 2015;24:24-33.
DOI:10.1016/j.jiec.2014.09.005

20. Imaga C, Abia A. Kinetics and mechanism of cadmium (II) ion sorption using carbonized and modified sorghum (sorghum bicolor) hull of two pore sizes (CMSH 150 um and 250 um). International Journal of Chemical and Process Engineering Research. 2015;2(4):44-58.
DOI:10.18488/journal.65/2015.2.4/65.4.44.58

21. Mohammad T, Choong C, Robiah Y, Suaraya A. Sorption kinetics for the removal of cadmium and zinc onto palm kernel shell based activated carbon. Journal Rekayasa Kimia Dan Lingkungan. 2010;7(4):149-155.

22. Wang S, Tang L, Bao Q, Lin M, Deng S, Goh M, Loh P. Room-temperature synthesis of soluble carbon nanotubes by the sonication of graphene xide. Journal of American Chemical Society. 2009;131(46):16832-16837.
DOI:10.1021/ja905968v

23. Mohammad R, Maoud A, Ali A, Mohammad R, Majid H, Syed R, Mohammad R. Flame atomic absorption spectrometric determination of Pb (II) and Cd (II) in Natural samples afetr column graphene oxide based solid phase extraction using 4-acetamidothiophenol. Journal of Brazilian Chemical Society. 2014;25(11):2063-2072.

24. Vilela D, Parmar J, Yongfei Z, Yanli Z, Samuel S. Graphene based microbots for toxic heavy metal removal and recovery

from water. Nano letters. 2016;16:2860-2866.
DOI:10.1021/acs.nanolett.6b00768

25. Wang Y, Liang S, Chen B, Guo F, Yu S, Tang W. Synergistic removal of Pb (II), Cd (II) and humic acid by Fe3O4 @ Mesoporous silica-graphene oxide composites. PlosONE. 2013;8(6).
DOI:10.1371/journal.pone.0065634

26. Riahi K, Chaabane S, Thayer B. A kinetic modeling of phospate adsorption onto phoenix dactylifera L. date palm fibers in batch mode. Journal of Saudi Chemical Society. 2017;1(21):S143-S152.
DOI:10.1016/j.jscs.2013.11.007

27. Cigden S, Yunus O. Error anlaysis studies of dye adsorption onto activated carbon from aqueous solutions. Particulate Science and Technology: An International Journal. 2014;32(1):20-27.
DOI:10.1080/02726351.2013.791360

28. Mahrouz A, Farzaneh S. Preconcentration of trace cadmium ion using magnetic graphene nanoparticles as an efficient adsorbent. Microchim Acta. 2014;181:181-188.
DOI: 10.1007/s00604-013-1094-4

29. Villanueva RAC, Hidalgo-Vazquez AR, Penagos CJS, Coretz-Martinez R. Thermodynamic, kinetic, and equilibrium Parameters for the removal of lead and cadmium from aqueous solutions with calcium alginate beads. Hindawi: The Scientific World Journal. Article ID 647512. 2014;1-9.
DOI: 10.1155/2014/647512.

30. Jiu-Hua D, Xiu-Rong Z, Guang-Ming Z, Ji-Lai G, Qiu-Ya N, Jie L. Simultaneous removal of Cd(II) and ionic dyes from aqueous solution using magnetic graphene oxide nanocomposite as an adsorbent . Chemical Engineering Journal. 2013;226: 189–200.
DOI: 10.1016/j.cej.2013.04.045.

31. Nkwoada A, Okoli K, Ekeanyanwu I. Novel kinetic modeling and optimization for adsorption of Zn2+ over graphene oxide. Journal of applied chemical science international. 2016;7(1):64-70.

32. Nkwoada AU, Simon O. Novel Dysprosium and Terbium Doped Taggants for Hydrocarbon Identification. Journal of Advanced Chemical Sciences. 2016;2(3): 296–298.

33. Bernard A. Cadmium and its adverse effects on human health. Indian Journal of Medical Research. 2008;128:557-564.

34. Dokmeci AC, Ongen A, Dagdeviren S. Environmental toxicity of cadmium and health effect. Journal of Environmental Protection And Ecology. 2009;10(1):84-93.

35. Jing X, Hongda L, Sheng-Tao Y, Jianbin L. Preparation of graphene adsorbents and their applications in water purification. De Gruyter: Review of Inorganic Chemistry. 2013;33(2-3):139-160.
DOI: 10.1515/revic-2013-007